# Melting and Premelting Transitions of an Oligomer Measured by DNA Base Fluorescence and Absorption†

Daguang Xu, Kervin O. Evans, and Thomas M. Nordlund*

*Department of Physics, University of Alabama at Birmingham, Birmingham, Alabama 35294-1170*

*Received November 23, 1993; Revised Manuscript Received May 5, 1994®*

ABSTRACT: Incorporation of 2-aminopurine (2AP) in place of adenine gives an optical probe of local and global DNA conformation. The temperature dependence of the absorption of the duplex d[CTGA(2AP)-TTCAG]$_2$ DNA decamer shows that the helix has approximately an all-or-none melting transition. Absorbance at wavelengths of 260 and 330 nm monitors the average normal base conformation and the 2AP base local conformation, respectively. From this measure, the 2AP base melts less than 1 °C below the other bases. Temperature-dependent lifetime measurements of 2AP also mirror the melting transition. Absorption spectra show that below $T_m$ most 2AP's are H-bonded. Fluorescence intensity and excitation spectra measurements show, on the other hand, that the most highly-fluorescent states correspond to non-H-bonded 2AP's which sense conformational changes of the helix. The temperature dependence of the fluorescence spectral shift shows the conformation and/or dynamics of the 2AP base changes 10 °C or more below $T_m$. The data suggest a premelting transition which is purely dynamic in nature—transient exposure of most 2AP's to water increases, while the average conformation remains B-helical.

Characterization of the cooperative melting transition is generally the first step in any physical or chemical study of DNA. The melting temperature, enthalpy, and entropy are usually expressed in terms of the all-or-none melting model (Bloomfield et al., 1974). In this model, if one base changes conformation, all bases follow suit. Many studies have shown that this is not always true in detail, but it is generally thought valid for DNA oligomer duplexes.

Direct testing of the nature of the melting transition demands experimental sensitivity to both global and local structural changes. We are developing the modified 2-aminopurine (2AP)[1] base into an optical probe of local structure in DNA. The absorption peak of this base, 305–315 nm, is well separated from those of the normal DNA bases (260–275 nm). DNA with an adenine base replaced by a 2AP base exhibits fluorescence which is easily observed at room temperature, as either a steady-state or time-resolved signal (Ward et al., 1969; Gräslund et al., 1987; Nordlund et al., 1989, 1990; Millar et al., 1990; Evans et al., 1992). Furthermore, substitution of adenine 5 by 2APs destroys neither the overall B-helical structure of a d(CTGAATTCAG)$_2$ duplex nor the specific recognition of the GAATTC sequence by the restriction endonuclease *Eco*RI (McLaughlin et al., 1987; Nordlund et al., 1989). 2AP can, in principle, be placed at any point in a DNA helix to monitor local events—conformational changes and binding to proteins, etc. The fluorescence signal from this probe can be observed even in the presence of large quantities of (nonfluorescent) DNA.

The all-or-none melting rule must, in fact, be violated in detail both for extremely long duplexes and for oligonucleotides. The melting temperature depends upon the relative GC base pair content of the helix (Bloomfield et al., 1974; Beers, 1967). Melting curves of λ DNA, for example, show numerous subtransitions within a broad melting profile and have been attributed to dissociation of different domains (Blake et al., 1981). In the case of short DNA, bases at the ends are more mobile and may have indistinct conformations below the melting temperature (Gueron et al., 1987). In the interior of an oligonucleotide, the bases may also undergo large motions while maintaining a time-averaged B-helical structure (Gräslund et al., 1987; Nordlund et al., 1989). Base mobility in general must increase as the melting transition is approached. In a previous study, we found the local motional rate (fluorescence anisotropy decay rate) of the 2AP base in the d[CTGA(2AP)TTCAG]$_2$ duplex to have activation energy of 8 kcal/mol over the temperature range 4–50 °C (Nordlund et al., 1989). No obvious evidence for a melting transition effect ($T_m$ = 23 °C) on the motional rate was evident. The amplitude of 2AP base motion from 4 to 25 °C was, however, smaller than at 30–50 °C, on average.[2]

Measurements and calculations of the probability of nucleic acid base pair opening and base pair proton exchange rates have clearly shown that enhanced base mobility occurs below the helix–coil transition temperature (Wilcoxon et al., 1984; Preisler et al., 1984; Wartell et al., 1985; Benight et al., 1988; Chan et al., 1990; Chen et al., 1991a,b, 1992). Analysis in this so-called premelting regime has centered on understanding proton exchange measurements. Several distinctions between "open", "exchangeable", and "premelting behavior" must be made in considering base pairs like A-T, 2AP-T, or A-U:

(i) the unstacked, non-H-bonded state of helix–coil transition theory;

(ii) the base pair "open" state, where all H bonds between two bases are broken;

(iii) the imino proton exchangeable state of N3 of A or 2AP;

† This research is based upon work supported by the National Science Foundation under Grant No. DMB 9118185.

® Abstract published in *Advance ACS Abstracts,* July 15, 1994.

[1] Abbreviations: 2AP, 2-aminopurine; A, adenine (6-aminopurine); C, cytosine; dA, deoxyadenylic acid; DNA, deoxyribonucleic acid; dT, deoxythymidylic acid; EDTA, ethylenediaminetetraacetic acid; G, guanine; poly[d(A-T)]·poly[d(A-T)], double-stranded deoxynucleic acid, each strand a polymer of alternating adenine and thymine bases; poly(dA)·poly(dT), double-stranded deoxynucleic acid, one strand a homopolymer of adenine and the other of thymine; T, thymine; Tris, tris(hydroxymethyl)aminomethane; UV, ultraviolet.

[2] See fluorescence anisotropy data in Table 2 of cited work. Uncertainties in the fitting of the multiexponential decay data in that work make detailed quantitation of the temperature dependence of motion amplitudes difficult.

0006-2960/94/0433-9592$04.50/0 

(iv) the amino proton exchangeable state of A (ring position 6) or 2AP (ring position 2);

(v) the premelting transitions monitored by CD, IR and Raman spectroscopy, UV fluorescence, singlet depletion anisotropy and electric birefringence decay, and gel mobility [see e.g., Brahms et al. (1976); Preisler et al. (1981, 1984); Chan et al. (1990); Nordlund et al. (1993)].

The distinction betweenh i, ii, and iii was shown by Benight et al. (1988). Apparently since the amino proton is normally accessible from the major groove, amino proton exchange (iv) can occur separate from i, ii, or iii (McConnell et al., 1984). Different physical mechanisms for transitions seen by CD, IR spectroscopy, and proton exchange are also seen in temperature dependences, where CD and IR spectroscopy showed significantly higher enthalpies (10–20 kcal/mol) than proton exchange (4–6 kcal/mol) (Preisler et al., 1981, 1984). Preisler et al. describe the IR- and CD-monitored premelting to be motions which are potential, but not productive, base pair-opening motions. It is possible that the 8 kcal/mol Arrhenius behavior of the motion of the 2-aminopurine base observed from fluorescence anisotropy (Nordlund et al., 1989) and the 17 kcal/mol premelting transition seen in spectral shifts (present work) and, previously, in the temperature dependence of energy transfer (Nordlund et al., 1993) parallel the differences between hydrogen exchange and CD and IR measurements.

The probability of a base pair "open" state, defined as an amino proton exchangeable state, can be significant in the premelting region. Chen et al. quote open probabilities of 1–6% for A-T base pairs, though the highest number was recently revised downward due to consideration of spine-of-hydration stabilization effects (Chen et al., 1991a, 1992). The apparent lower stability of the 2AP-T base pair (McLaughlin et al., 1987) suggests that its open probability in our DNA B-helix will be at least that high. This premelting transition is also expected to be cooperative in the d[CTGA(2AP)-TTCAG]$_2$ duplex, as the cooperative unit for CD-detected premelting of poly[d(A-T)] was shown to be less than 10 base pairs (Gennis et al., 1972).

Increased mobility of a base results in a base environmental change even if the average structure still conforms to B-helical parameters. This is because the base will transiently be exposed to a wider variety of neighboring molecular conformations, both from the DNA and from the solvents molecules. Optical spectroscopy can sense this environmental change. Fluorescence and absorption spectra shift as the polarity of the 2AP base environment changes (Smagowicz et al., 1974; Kawski et al., 1975; Bierzynski et al., 1977; Evans et al., 1992). The process of absorption occurs from the equilibrium ground state on a time scale of about $10^{-15}$ s, so a mobile base fluctuating in conformation on time scales of $10^{-13}$ s or slower will have an absorption spectrum corresponding to an instantaneous snapshot of all the environments. Steady-state fluorescence spectra are different. The fluorescence decay time of a free 2AP base surrounded by water is 10 ns, while that in an oligomer ranges from subnanosecond to about 10 ns (Gräslund et al., 1987; Nordlund et al., 1989; Millar et al., 1990). If the base samples various environments, the average fluorescence excitation (or emission) spectrum will be more highly weighted by the spectrum of the long-lived fluorescence decay structure—that of the water-exposed conformation. The extent of the shift will depend upon the average residence times (or populations) in the various conformations. If, for example, two conformations have relative populations, fluorescence decay times, and fluorescence peak positions of 90%, 0.5 ns, 360 nm and 10%, 10 ns, 370 nm and if fluorescence yield scales decay with time,[3] the relative weighting of the spectrum of the minority 370-nm species to the majority 360-nm species will be (0.1 × 10 ns):(0.9 × 0.5 ns) = 2.2:1 under conditions of slow interconversion. The fluorescence excitation spectrum will shift to that of the minority species as the base becomes mobile even though the average conformation has not similarly shifted. Mobility is governed by temperature, and this type of spectral shift can occur even in the absence of a melting transition.

A temperature-induced structural transition can also induce a spectral shift. In this case, as temperature is increased, the melting transition will allow a change in the average exposure of the bases to water. This spectral shift should then mirror, approximately, the melting transition.

Steady-state fluorescence intensity of the 2-aminopurine-modified DNA duplex decamer vs temperature shows a complex behavior as a function of temperature, increasing from low temperature up to the melting temperature and then decreasing rapidly at high temperature (Gräslund et al., 1987; Nordlund et al., 1990; Wu et al., 1990). In the second reference, the time-resolved fluorescence decay components, obtained by fitting four exponential decay components to the data, were integrated over time. If amplitudes of fluorescence decay components [$a_i$ in the fitting expression $I(t) = \sum a_i \exp(-t/\tau_i)$] correspond to slowly-interconverting populations of conformers which participate in the melting transition, then plotting component amplitudes vs temperature might be expected to display the melting transition. No such behavior is apparent from the fitting parameters (Nordlund et al., 1989, 1990). It is likely that either the fitting expression is not physically appropriate, it mixes together the real conformers, or the interconversion is not slow compared to fluorescence lifetimes. Considering the local mobility of the DNA, a model incorporating a continuous distribution of fluorescence decay populations may be physically more appropriate. Models incorporating such distributions show some promise to clarifying the connection between populations of fluorescence decay components and structural conformers (not shown).

Our present data on the melting of 21 μM d[CTGA(2AP)-TTCAG]$_2$ DNA duplex in 0.1 M NaCl, 0.1 mM EDTA, 10 mM Tris-HCl buffer, pH 7.5, show that the melting transition occurs at 28.4 ± 0.8 °C when measured by absorption of either normal bases or 2AP base, with the 2AP base possibly melting only 0.3 °C earlier than the other bases. A plot of the thermal quenching rate of the longest lifetime in the multiexponential fluorescence decay also suggests a melting transition, but the midpoint of the transition is apparently shifted several degrees higher. In contrast, a fluorescence excitation spectral transition occurs and completes itself well below the melting transition.

## MATERIALS, METHODS, AND ANALYSIS

*Absorption Spectra and Hypo/Hyperchromism.* The d[CTGA(2AP)TTCAG]$_2$ decamer was prepared as described (McLaughlin et al., 1988). Absorption spectral measurements were performed with samples of duplex concentration 3–4, 10, and 21 μM. Absorption spectra were measured on a Gilford Response or Response II spectrophotometer, using a

[3] Quantum yield: $\phi = \tau/\tau_0$, where $\tau$ is the observed, average lifetime and $\tau_0$ is the radiative lifetime. This is normally observed to be the case as long as instrumentation is capable of resolving all fluorescence decay components. Since the radiative lifetime is proportional to the integrated extinction coefficient, base hypochromism can cause changes in $\tau_0$. These changes are typically 15–30%.

1-nm bandwidth. A 1.0-mm path length cuvet was used for the 21 μM measurements at 260 nm. Path lengths otherwise were 1.0 cm for absorbance. Data were stored digitally and transferred to a computer for analysis and plotting.

Melting curves measured by absorption were performed in the Gilford spectrometers using the programmable thermoelectric temperature controller. The samples were placed in stoppered 0.3- × 1.0-cm (or × 0.1-cm) path length cells, heated to 70 °C to preclude later air bubble formation, and cooled slowly to the lowest temperature, at which point the programmed heating was begun. Heating rates were 1 °C/min. The wavelength was set at 260 nm for normal bases, where absorption increases with increasing temperature. 2AP base absorption was measured at 330 nm; a decrease of absorption with temperature is observed. A wavelength of 330 nm was chosen for comparison with previous results (Eritja et al., 1986) and because it minimizes the overlap with absorption bands of normal bases. The 2AP absorption decrease with temperature at 330 nm has two contributors: base hypochromism and the blue shift of the absorption spectrum as temperature rises, the latter predominating at 330 nm (Eritja et al., 1986; present results).

*Fluorescence Measurements.* Fluorescence lifetime data are from oligonucleotide samples of duplex concentration 5 μM. Fluorescence spectra were collected using a Perkin-Elmer LF-50 fluorometer. Excitation and emission bandwidths were 2.5 and 5 nm, respectively. Data were stored, converted to ASCII, and transferred to the computer for plotting and manipulating. Displayed excitation spectra are corrected for lamp intensity fluctuations and detector wavelength dependence.

*Fluorescence Lifetimes.* Fluorescence lifetime data of the d[CTGA(2AP)TTCAG]$_2$ decamer are taken directly from Nordlund et al. (1989). Time-resolved fluorescence decays of the 2AP free base in water were measured with a time-correlated single-photon counting apparatus in the Department of Chemistry of the University of Rochester (Wu et al., 1990). A rhodamine 6G dye laser, frequency doubled to 300 nm, was synchronously pumped by a frequency-doubled, continuous wave mode-locked neodymium:YAG laser system. Fluorescence was detected with a cooled, UV sensitive Hamamatsu microchannel plate photomultiplier system. Under experimental conditions, the system response time was 100 ps, full width at half-maximum.

*Analysis of Absorption Data.* Absorption melting curves were fitted with two programs, generously provided respectively by D. H. Turner [University of Rochester (Frier et al., 1983)] and D. Muccio and F. Fish [University of Alabama at Birmingham (Muccio et al., 1992)]. The latter program employed either linear or quadratic temperature dependence of the absorbance at the high- and low-temperature limits and gave thermodynamic parameters which were within error bars shown in the data. Results from the two programs also agreed with each other within error bars. Melting temperatures were calculated from the temperature of the maximum slope of absorbance vs $1/T$ and from the simultaneously-fitted enthalpy and entropy. Fits were done by simultaneously fitting the shape and position of the curve, including the slopes of the lines far above and below the melting temperature.

*Analysis of Fluorescence Spectral Shifts.* Spectral bands can be characterized by the position of spectral peaks or by variously-defined average wavelengths, wavenumbers, or energies. The precision to which such a spectral maximum average can be determined is limited by spectral width and noise. In our case of fluorescence excitation spectra, the full spectral width is 40–50 nm, with some overlap of a higher-energy excitation band at short wavelength. Under these circumstances, it is difficult to resolve the position of the band to better than about 1 nm. However, the method of difference spectroscopy allows for much more precise determination of the *shift* of a spectral peak. If two broad spectra differ by a wavelength shift very small compared to their width, subtraction of the two spectra results in a difference spectrum whose maximal amplitude is proportional to the shift. This difference amplitude can then be used to determine the shift. The proportionality factor depends upon the shape of the spectrum. It can easily be calculated for a Gaussian spectrum, but numerical methods, using the average shape of the actual spectra, are more accurate. We therefore determined the shift proportionality factor by first constructing a spectrum consisting of the average of all of the measured spectra, normalized in maximum amplitude to 1.0. This spectrum represents the true, average spectrum, with no assumptions as to shape except that the shape is assumed not to change significantly in the region where difference amplitude is used to calculate the shift. Small wavelength shifts are then artificially imposed on the spectrum, and the average spectrum is subtracted from the shifted spectra. These difference spectra will have a positive and negative maximum on either side of the average spectrum's peak. The imposed wavelength shift (in nanometers) is then plotted as a function of the difference amplitude. The slope of this plot is the proportionality factor between difference spectral amplitude and wavelength shift. In the present case, this proportionality factor is

$$\text{shift (nm)} = 28.1\Delta I$$

where $\Delta I$ is the difference between the (normalized) spectrum measured at temperature $T$ and the reference spectrum. Real shifts of the spectrum can then be determined by applying the shift equation to measured spectra which are shifted as a result of physical changes, e.g., temperature. The reference spectrum can be an average spectrum, as described above, or the spectrum at some meaningful reference temperature, such as the high-temperature limit. We choose our reference spectrum, as that measured at 50 °C, where the helix is mostly single-stranded. The difference is calculated as the average difference at 324–326 nm, near the longer-wavelength difference spectral peak. The net result of this analysis is that though the exact position of the spectral peak at any temperature may not be known to better than ±0.5 nm (or worse), the *shift* of that peak from that of a reference spectrum can be precisely measured. We conservatively quote the error of the shift at ±0.2 nm.

It is important to note that the above analysis applies to a spectrum which is truly shifting with temperature. If the observed spectrum consisted of a temperature-dependent weighted sum of two spectra centered at 315 and 305 nm, for example, the spectral width and shape would change considerably with temperature. This is not the case with the present data (Evans et al., 1992; Nordlund et al., 1993).

*Analysis of Time-Resolved Fluorescence.* Fluorescence lifetimes are also expected to sense the helix–coil transition of an oligonucleotide. Below the melting temperature, a base has some mobility and can occupy a restricted number of conformations. As the helix melts, new conformations become accessible, both to the base and to the remainder of the DNA structure. The base is no longer restricted by hydrogen bonding to its partner on the opposite chain and probably is less restricted by stacking interactions. If one makes a simple model of the helix as in Figure 1, one expects the quenching

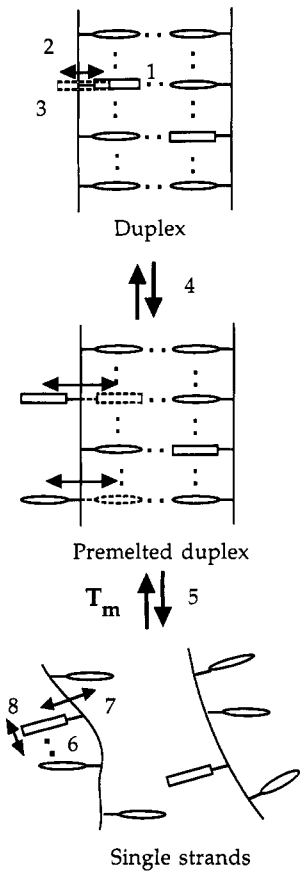


FIGURE 1: Model for structure and dynamics in the DNA duplex, premelted duplex, and melted coil. 1: Average base conformation is stacked, H-bonded form; fluorescence is weak (short decay time). 2: Base motion evident—proton exchange, fluorescence anisotropy decay, molecular dynamics simulations. 3: A small fraction of bases are not H-bonded and are responsible for most fluorescence. These encounter only ~8 kcal/mol barrier to motion. The state does not have to be completely unstacked but must be more exposed to water and proton exchangeable. 4: Premelting region. As temperature rises, motion of bases increases rapidly starting 10–15 °C below $T_m$, hindered by ~17 kcal/mol activation barrier caused by H bonding and stacking. Average structure is still B-helical. 5: Melting transition, duplex → single strand. All H bonds broken. 6: Stacking interactions still exist in single strand. 7: Base motion occurring, still with ~8 kcal/mol activation barrier. 8: Motion of DNA causes fluorescence quenching at high temperature.

of fluorescence of the most water-exposed state to increase upon helix melting. The state of the 2AP base of Figure 1 (see note 3 of figure caption) may correspond to the proton exchangeable state of NMR measurements (Lycksell et al., 1987; Gueron et al., 1987). We make the assumption that the most water-exposed conformer is identified as the state with a fluorescence lifetime nearest that of the free 2AP base in water, 10 ns. The quenching of this (relatively rarely-occurring) state by collision or near-approach of neighboring DNA structure in the duplex is restricted by the ordered structure of the helix. When the helix melts, molecular groups in the DNA structure have freer access to the 2AP base, increasing the quenching rate (Figure 1, notes 6–8). If one then plots the temerature dependence of the lifetime of this fluorescence component, one should see evidence of the melting transition. We must, however, account for the intrinsic temperature dependence of the free 2AP base lifetime in water. We do this by dividing the oligonucleotide's longest fluorescence lifetime by the lifetime of the free base at the same temperature. This procedure has the same effect as removing the base line slope of an absorption vs $T$ curve at temperatures well below and above $T_m$ in the more standard, hypochromic melting curve measurement. The mathematical justification for this follows. Note that the fraction of bases exposed to water does not enter into this argument. The long-lived fluorescing base is a minority species and may act as a "voyeur", observing the conformation of the oligonucleotide and responding to that by altering its fluorescence lifetime.

We treat the temperature dependence of fluorescence lifetime by first determining the longest-lived decay component. This has already been done (Nordlund et al., 1989). We choose this component because its measured temperature dependence is simplest. (In our model, we will identify this component as the water-exposed conformation of Figure 1.) The decay rate of the excited-state corresponding to this longest-lived component is the sum of the radiative decay ($k_r$), nonradiative decay ($k_t$, temperature-dependent intramolecular or solvent-coupled de-excitation), and quenching decay rates ($k_q$). $k_q$ is presumably caused by the presence of nearby DNA structure. The fraction, $f$, of the fluorescence decay component which is quenched is given by

$$f = k_q/(k_r + k_t + k_q)$$

The decay rate of the 2AP free bases is just $k_r + k_t$, while $k_r + k_t + k_q$ = the decay rate of 2AP in the decamer. $f$ can then be written as

$$f = 1 - \tau_{dec}/\tau_{fb}$$

where $\tau_{dec}$ ($\tau_{fb}$) is the excited-state lifetime of 2AP in the decamer (free base in water). This quenched fraction should depend upon two factors: (i) melting of the DNA, which facilitates quenching, and (ii) the intrinsic temperature dependence of the quenching rate in the exposed state. The latter is presumably dependent on the temperature-dependent motions of DNA structure near the 2AP base. If ii had a negligible temperature dependence compared to the melting transition, then $f$ would exactly mirror the melting transition and exhibit an s-shaped curve centered about $T_m$ when plotted vs $T$. If ii is appreciable and the quenching (molecular motion) increases with temperature, then $f$ would still be s-shaped but the midpoint temperature would be shifted higher.

## RESULTS

*Absorption at 260 and 330 nm vs T.* The curves describing absorption of normal bases (260 nm) and 2AP (330 nm) vs temperature in the 21 μM d[CTGA(2AP)TTCAG]$_2$ decamer are almost mirror images of each other about a horizontal plane (Figure 2). The total percent change in absorption at 260 nm is about 14%, while that at 330 nm is near −50%. The latter is considerably larger than expected from simple hyperchromism. The shift of spectrum to shorter wavelengths with increasing temperature constitutes a large portion of this change and has been correlated with breaking of the 2AP-T H bond (Sowers et al., 1986). The midpoint of the curve can be found near 28 °C. This agrees with the previously-reported value of 32 °C (McLaughlin et al., 1987) when account is made of the differing ionic strengths. Both of these values are approximately 10 °C lower than the melting temperature of the decamer with adenine in position 5 (data not shown).

Computer fitting of the curves in Figure 2 simultaneously for the low- and high-temperature slopes ($\Delta\epsilon/\Delta T$), $T_m$, entropy ($\Delta S$), and enthalpy ($\Delta H$) of the transition, and calculation of $T_m$ corresponding to the maximal slope of an absorbance vs $1/T$ plot confirm the $T_m$ estimate from the midpoint of the plot but suggest a 0.3 ± 0.5 °C lower melting temperature at 330 nm than the 260 nm (Table 1). A previous study of the

Table 1: Melting Temperatures, Enthalpies, and Entropies for d[CTGA(2AP)TTCAG]$_2$[a]

| method | solution[a] | $T_m$ (°C)[b] | $\Delta H$ (kcal/mol) | $\Delta S$ (cal/K mol) |
|---|---|---|---|---|
| A (260 nm) | 21 μM; 0.1 M KCl, 0.1 mM EDTA | 28.3 ± 0.5 | −57 ± 1 | −169 ± 3 |
| | 3–4 μM; 0.1 M KCl, 0.1 mM EDTA | 20.4 ± 1.5 | −34 ± 2 | −92 ± 6 |
| | 3–4 μM; 0.2 M KCl, 20 mM $MgCl_2$ | 32.2 ± 1.5 | −49 ± 1 | −137 ± 2 |
| A (330 nm) | 21 μM; 0.1 M KCl, 0.1 mM EDTA | 28.6 ± 1.0 | −63 ± 3 | −186 ± 10 |
| fluor lifetime[c] | 3–4 μM; 0.1 M KCl, 0.1 mM EDTA | 28 | – | – |
| calculated[d] | | | −65 | −166 |

[a] Enthalpies and entropies per mole of single strand. Solutions contain 10 mM Tris-Cl, pH 7.5. Oligonucleotide concentration (μM) listed is duplex concentration. [b] Absorbance-derived $T_m$ is average of $T_m$ determinations from (i) maximum derivative of curve with respect to $1/T$, (ii) enthalpy, entropy, and concentration relation, and (iii) the temperature at which slope of absorbance vs $T$ reaches its maximum × 0.971. Error bars reflect standard deviation of $T_m$ from these three methods, not reproducibility of data. [c] From fluorescence lifetime plot. See text. [d] Method of Breslauer (Breslauer, 1986) for adenine-containing oligomer.

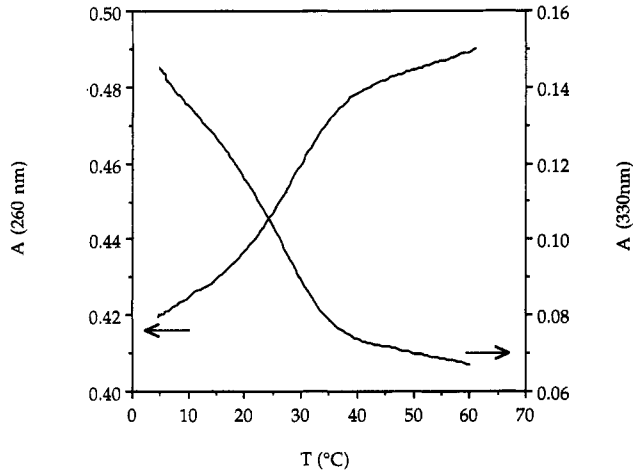


FIGURE 2: Melting curves for the d[CTGA(2AP)TTCAG]$_2$ decamer (21 μM) measured by absorption vs temperature at 260 and 330 nm. A wavelength of 260 nm monitors the normal base absorption, while that at 330 nm measures only the change in 2AP absorption. Correction for buffer absorbance vs $T$ has been made. Path length 1.0 cm for 330 nm and 0.1 cm for 260 nm.

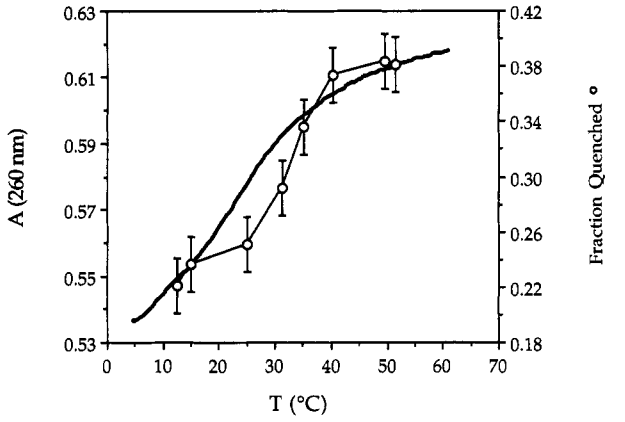


FIGURE 3: Melting curves for the 4 μM d[CTGA(2AP)TTCAG]$_2$ decamer measured by temperature dependence of 260-nm absorption and of the quenched fraction. The quenched is calculated from data reported in Nordlund et al. (1989) and from time-resolved, single-exponential fluorescence decays of the free base in water (data not shown). The fraction is calculated as $1 - \tau_{dec}/\tau_{fb}$, where $\tau_{dec}$ is the lifetime of the longest-fluorescence decay component of the decamer and $\tau_{fb}$ is the lifetime of the free base. See text. Also shown are 260-nm absorbance measurements for comparison.

melting of oligonucleotides with incorporated 2AP reported a 2–3 °C lower value of $T_m$ when measurements were done at 330 nm (Eritja et al., 1986). Our 0.3 °C difference is smaller and within the uncertainty of the computer fit. The enthalpies in Table 1 likewise show no evidence that the 2AP-T base pair is less stable than the other, normal base pairs. 2AP does destablize the helix, since $T_m$ is 10 °C lower than that of the d(CTGAATTCAG)$_2$ oligonucleotide, but the destabilization apparently extends over the entire helix.

*Fluorescence Lifetime vs Temperature.* Figure 3 shows a plot of fluorescence-quenched fraction vs temperature for the longest-lived fluorescence decay component of the 5 μM 2AP decamer, as described in the analysis section, together with a standard 260-nm absorption melting curve. The former curve displays the sigmoidal shape expected from a melting transition, but the midpoint temperature is apparently higher. Comparison of the two curves also suggests the slope of the lifetime plot is greater than that of the absorption vs $T$ plot. The small number of fluorescence data points in Figure 3 and the error intervals of the lifetime values from computer fits make the corresponding enthalpy and entropy estimates uncertain.

*Fluorescence Spectra vs Temperature.* Simultaneous with the absorption changes vs temperature is a steady-state fluorescence intensity change. Figure 4 shows that this fluorescence change can be determined from an excitation spectrum vs temperature plot. Two changes are obvious from this plot. First, the intensity increases from low temperature to approximately the melting point and then decreases above the melting temperature. This result is consistent with those

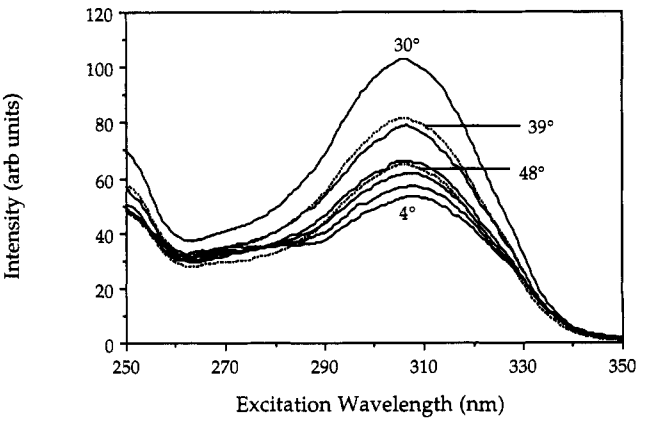


FIGURE 4: Change of the fluorescence excitation spectrum of d[CTGA(2AP)TTCAG]$_2$ with temperature. The corrected spectra are plotted for temperatures between 6 and 48 °C. The intensity of the spectra increases with temperature up to about 30 °C and then decreases. The spectra also shift to the blue with increasing temperature (Figure 5).

reported earlier, where emission spectra or wide-bandwidth emission intensities vs temperature were determined (Gräslund et al., 1987; Nordlund et al., 1990). Second, close examination of the plots also reveals a blue shift of the spectrum with increasing temperature, which we noted (Evans et al., 1992). We present here a more complete set of data, extending to lower temperature and at three differing concentrations, along with improved analysis of the shift. (See the methods section.) Figure 5 shows (i) that the functional form of the

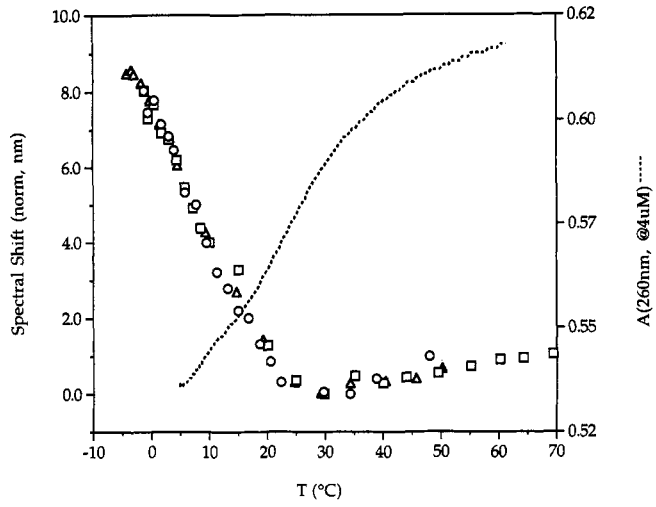


FIGURE 5: Shift of the fluorescence excitation spectrum maximum of 4 (○), 10 (□), and 21 (△) μM duplex d[CTGA(2AP)TTCAG]$_2$ with increasing temperature. The magnitudes of the shifts have been normalized by multiplying by 1.95, 1.40, and 1.00, respectively, at 4, 10, and 21 μM. Also plotted is the 260-nm absorption vs $T$ curve for the 4 μM duplex. Fluorescence emission was monitored at 370 nm.

spectral shift is duplex concentration independent and (ii) that this blue shift occurs well below the melting temperature. The maximum amplitude of the spectral shift depends, however, on concentration. The maximal shifts have been normalized to that at 21 μM, the shifts at 4 and 10 μM being 1.95 and 1.4 times smaller than that at 21 μM. The absorbance vs temperature curves, on the other hand, shift to higher temperature with increasing concentration. See figure caption and McLaughlin et al. (1988). The shift occurs primarily between −2 °C (and probably below) and about 22 °C; between 22 and 30 °C, the blue shift continues but with much reduced temperature dependence. Above 30 °C, the spectral shift direction changes back toward the red, though again with reduced temperature dependence. This temperature dependence mimics that found for energy transfer efficiency from normal to 2AP base (Nordlund et al., 1993). The rapid fluorescence intensity decrease, in contrast, continues well beyond 40 °C. Absorbance at 260 nm similarly exhibits a stronger temperature dependence than the spectral shift above 30 °C. The absence of an isosbestic point is related to the small energy transfer band in the 250–290-nm region (Nordlund et al., 1993).

The fluorescence emission spectrum of the decamer changes very little in position with temperature (Figure 6), in contrast to the excitation spectrum. The difference in peak position is about 1 nm, comparing the spectra at 4 and 50 °C.

## DISCUSSION

*The All-or-None Principle.* The all-or-none principle predicts that the melting curves measured at 260 nm (absorption of all bases besides 2AP) and 330 nm (absorption of 2AP) should be identical. Our results show that the d[CTGA(2AP)TTCAG]$_2$ decamer melts at about 28 °C and that the 2AP base undergoes a melt, at most, about 0.7 °C below that. The all-or-none principle thus holds to the extent that when the 2AP base melts, all the other bases also melt. These results contrast somewhat with previous studies on other 2AP-containing oligomers, which showed a 2–3 °C lower transition temperature from the 2AP absorption than from 260-nm absorption (Eritja et al., 1986). These latter results were obtained from the temperature corresponding to the maximum slope of an absorption vs temperature plot.

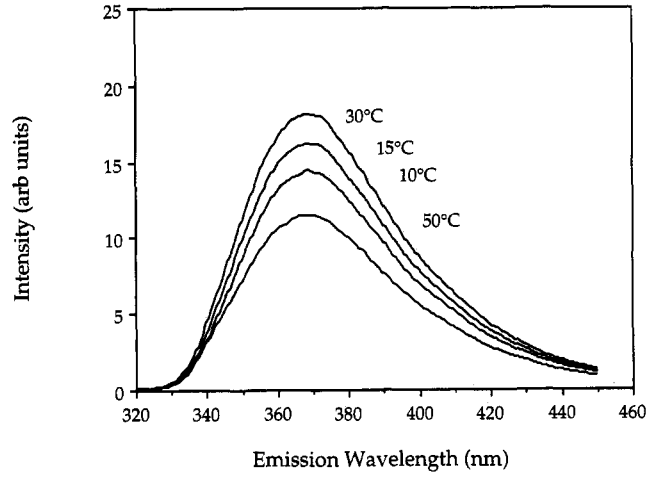


FIGURE 6: Fluorescence emission spectrum of d[CTGA(2AP)-TTCAG]$_2$ vs temperature. The spectral peak position at high temperature is at most 1 nm to the red of that at 4 °C.

*What Does 2AP Fluorescence Sense?* 2AP bases can probably exist in a continuum of states, ranging from base-paired, stacked bases to unpaired, unstacked bases, depending upon solvent conditions and thermodynamic parameters. The environments of these base states can range from relatively hydrophobic, inside the helix, with considerable interaction with nucleotides, to hydrophilic, extensively surrounded by water. The absorption of 2AP is moderately sensitive to these environmental changes. Shifts in absorption of 1–10 nm can occur, and the strength of the absorption may change by 10–40% due to hypochromic effects. The absorption peak of 2AP in the decamer below the melting temperature is near 315 nm (Evans et al., 1992), consistent with other data on shorter 2AP-containing oligonucleotides (Eritja et al., 1986; Goodman et al., 1983). This absorption peak corresponds to the protonated form of N1 in the 2-aminopurine ring (Sowers et al., 1986), consistent with the double-H-bond model of base pairing of 2AP with thymine. When the helix melts or when the 2AP free base is dissolved in water near neutral or high pH, there is no aminopurine N1 H bond and the absorption peak is near 305 nm (Evans et al., 1992; Eritja et al., 1986; Goodman et al., 1983; Gryczynski et al., 1977; Smagowicz et al., 1974). The fluorescence excitation spectrum of the 21 μM d[CTGA(2AP)TTCAG]$_2$ decamer, on the other hand, peaks near 315 nm only at the extreme low-temperature region, −2 °C or below, the shifts to 309 nm by about 10 °C and to 306 nm by about 20 °C, i.e., still below the absorbance-measured melting transition [Evans et al. (1992) and this work]. The simplest conclusions from these evidences are (i) the majority of 2AP bases are normally base-paired in the duplex at low temperature, as shown by the absorption peak near 315 nm; (ii) the majority of 2AP bases are not base-paired in the DNA at high temperature, as shown by the absorption and fluorescence excitation peaks near 305 nm; and (iii) the 2AP fluorescence comes primarily from 2AP bases which are not base-paired. The last statement is based on the difference in peak position between the fluorescence excitation spectrum and the absorption spectrum at temperatures (10–30 °C) where the fractions of both unmelted and melted forms are non-negligible. It has been noted that the fluorescence yield of 2AP in DNA is an order of magnitude lower than that of the free base and that the fluorescence decay is highly nonexponential, with components ranging in decay time from less than 100 ps to 10 ns, the latter about equal to that of the free base in aqueous solution near neutral pH (Nordlund et al., 1989; Millar et al., 1990; Evans et al.,

1992). It now appears that a primary case of the rapid decay (low fluorescence yield) components is base pairing. Measurements by Ward et al. foreshadowed these conclusions (Ward et al., 1969).

*Spectral Shifts and Premelting Behavior.* The fluorescence excitation peak of d[CTGA(2AP)TTCAG]$_2$ shifts to the blue as temperature rises from −2 to about 22 °C and remains comparatively constant at higher temperatures. This blue shift is consistent with 2AP exposure to a higher-polarity environment. The surprising observation is, however, that this spectral shift is completed before the midpoint of the melting curve is reached. Since this kind of spectral shift is not observed for the free base in solution, one must conclude that a conformational change takes place in the DNA before the melting transition occurs—a premelting transition. Since the spectrum is specific to the 2AP base alone, we can conclude, in particular, that the environment (i.e., the rest of the helix) of the 2AP base in position 5 of the d[CTGA(2AP)TTCAG]$_2$ duplex is changing. The fact that the 2AP 330-nm absorbance vs $T$ curve, caused primarily by the shift of the 2AP absorption spectrum from 315 to about 305 nm (breaking of the 2AP-T H bond), has its midpoint close to the $T_m$ of the normal bases seems to contradict this, however, unless the premelting transition does not constitute a change in the time-averaged structure of the oligonucleotide, on which the absorption spectrum depends. We prepose that the 2AP base becomes significantly more mobile 10 °C or more below the melting temperature. This increased mobility allows increased exposure to water, whose high polarity causes a blue spectral shift in the fluorescence excitation spectrum.

The concentration dependence of the premelting shift shows that the transition involves the duplex form of DNA, as the shape of the shift vs $T$ curve remains fixed and the maximal shift increases with increasing concentration. This would not be expected if, for example, a single-stranded hairpin struture were the source of the "premelting transition". Hairpin structures are also unlikely because they would leave the 2AP base in a non-base-paired region whose exposure to water would be temperature independent, resulting in little spectral shift. The trend of the spectral shift data (larger shifts for higher concentrations) and the thermodynamic data of Table 1 suggest that at 4 μM duplex concentration with 0.1 M KCl and no $MgCl_2$, the helix is indeed double but less stable and more mobile. At 21 μM, the observed thermodynamic data (Table 1) agree well with the calculated data, confirming the identification of duplex DNA.

*A Model.* Figure 1 is the starting point for our model. The double-helical structure predominates at temperatures well below $T_m$. However, the 2AP base (like any base!) can transiently break its hydrogen bond with its base pair partner, as has been demonstrated by proton exchange (Gräslund et al., 1987; Lycksell et al., 1987). The fraction of bases which are "open" at any time is small and can be estimated (Chen et al., 1991a, 1992). At very low temperature (≤2 °C), the mobility of bases is low and the fluorescence excitation spectral peak coincides with the absorption peak, 315 nm (21 μM sample). The energetic barrier to motion of these open bases as detected by fluorescence anisotropy decay time (~8 kcal/mol; Nordlund et al., 1989) does not have a contribution from base pair hydrogen bonds. As temperature rises from −2 °C, a premelting thermodynamic transition takes place that allows (i) the motions to become more extensive and (ii) more bases to undergo these motions. The latter necessitates an additional ~9 kcal/mol to disrupt hydrogen bonds. This transient excursion toward increased solvent exposure is still rare enough that the average conformation of the 2AP is B-helical. When a base becomes more exposed to water and the base pair H bonds break during its outward travels, it sees an environment much like that of the free base in water. Two of these properties are blue-shifted fluorescence excitation spectrum and long fluorescence lifetime. The long fluorescence lifetime can be observed at all temperatures, though the fraction is low. (The other shorter-fluorescence lifetime components result from the much more complex interactions of the 2AP base when it is not so exposed to water and closer to other parts of the DNA structure.) When the temperature rises above $T_m$ and the predominant structure is nonduplex, the structure of the DNA becomes less ordered and more flexible. This allows quenching of the 2AP fluorescence via collisions with adjacent atoms on the chain. This dynamic quenching allows Figure 3 to roughly reflect the melting transition.

*Implications for DNA Interactions.* A dynamic premelting structural transition in DNA which has little effect on the time-averaged structure would seem at first glance to have no relevance for DNA interactions. The developing realization of the importance of structural dynamics in proteins is transferring to the case of nucleic acids, however, with which many proteins interact (Westhof et al., 1987; Chan et al., 1990). Early models of protein interactions with substrates centered on a lock-and-key model, in which the substrate exactly and rigidly fit into a rigid "keyhole" at the active site of the protein. NMR measurements on the structures of small proteins have produced more and more cases of the complete nonexistence of a defined 3D structure at an active site, which then becomes ordered upon binding. See, e.g., Adler et al. (1993). One might suspect that DNA is similar. The GAATTC sequence contained in modified form in our oligonucleotide constitutes the recognition sequence of the *Eco*RI protein. X-ray crystallography shows a distorted helix in this sequence when bound to the protein (Frederick et al., 1984; Rosenberg et al., 1986; Kim et al., 1990). The distortion either does not exist or exists in some other form in the unbound DNA (Rosenberg et al., 1986; Thomas et al., 1989; Nerdal et al., 1989). DNA, in particular the DNA we are investigating, must have the capability to undergo transient structural transitions which facilitate interaction with proteins. A dynamic structural transition of the type we report, which does not involve an energetically-expensive, average conformational change but which allows the DNA to rapidly explore conformations conducive to interaction with proteins well below the melting temperature, would seem to fit nicely the demands of protein–DNA recognition.

## ACKNOWLEDGMENT

The authors gratefully acknowledge the efforts of L. W. McLaughlin and co-workers in the synthesis and characterization of the DNA decamers and the early input of R. Rigler and L. Nilsson into structural and motional characterization of DNA.

## REFERENCES

Adler, M., Carter, P., Lazarus, R. A., & Wagner, G. (1993) *Biochemistry 32*, 282–289.

Beers, W. (1967) *Proc. Natl. Acad. Sci. U.S.A. 58*, 1624.

Benight, A. S., Schurr, J. M., Flynn, P. F., Reid, B. R., & Wemmer, D. E. (1988) *J. Mol. Biol. 200*, 377–399.

Bierzynski, A., Kozlowska, H., & Wierzchowski, K. L. (1977) *Biophys. Chem. 6*, 213–222.

Blake, R. D., Vosman, F., & Tarr, C. E. (1981) in *Biomolecular Stereodynamics* (Sarma, R. H., Ed.) pp 439–458, Adenine Press, New York.
Bloomfield, V., Crothers, D., & Tinoco, J. I. (1974) *Physical Chemistry of Nucleic Acids*, Harper & Row, New York.
Brahms, S., Brahms, J., & Van Holde, K. E. (1976) *Proc. Natl. Acad. Sci. U.S.A. 73*, 3453–3457.
Breslauer (1986) *Proc. Natl. Acad. Sci. U.S.A. 83*, 3746–3750.
Chan, S. S., Breslauer, K. J., Hogan, M. E., Kessler, D. J., Austin, R. H., Ojemann, J., Passner, J. M., & Wiles, N. C. (1990) *Biochemistry 29*, 6161–6171.
Chen, Y. Z., & Prohofsky, E. W. (1992) *Nucleic Acids Res. 20*, 415–419.
Chen, Y. Z., Feng, Y., & Prohofsky, E. W. (1991a) *Biopolymers 31*, 139–148.
Chen, Y. Z., Zuang, W., & Prohofsky, E. W. (1991b) *Biopolymers 31*, 1273–1281.
Eritja, R., Kaplan, B. E., Mhaskar, D., Sowers, L. W., Petruska, J., & Goodman, M. F. (1986) *Nucleic Acids Res. 14*, 5869–5884.
Evans, K., Xu, D.-G., Kim, Y.-S., & Nordlund, T. M. (1992) *J. Fluoresc. 2*, 209–216.
Frederick, C. A., Grable, J., Melia, M., Samadzi, C., Jen-Jacobson, L., Wang, B.-C., Greene, P., Boyer, H. W., & Rosenberg, J. M. (1984) *Nature (London) 309*, 327.
Frier, S. M., Albergo, D. D., & Turner, D. H. (1983) *Biopolymers 22*, 1107–1131.
Gennis, R. B., & Cantor, C. R. (1972) *J. Mol. Biol. 65*, 381–399.
Goodman, M. F., & Ratliff, R. L. (1983) *J. Biol. Chem. 258*, 12842–12846.
Gräslund, A., Claesens, F., McLaughlin, L. W., Lycksell, P.-O., Larsson, U., & Rigler, R. (1987) in *Structure, Dynamics and Function of Biomolecules* (Ehrenberg, A., Rigler, R., Gräslund, A., & Nilsson, L., Eds.) pp 201–207, Springer-Verlag, Berlin.
Gryczynski, I., & Kawski, A. (1977) *Bull. Acad. Pol. Sci., Ser. Sci., Math. Astron. Phys. XXVI*, 1189–1195.
Gueron, M., Kochoyan, M., & Leroy, J. L. (1987) in *Structure, Dynamics and Function of Biomolecules* (Ehrenberg, A., Rigler, R., Gräslund, A., & Nilsson, L., Eds.) pp 196–200, Springer-Verlag, Berlin.
Kawski, A., Bartoszewicz, B., Gryczynski, I., & Krajewski, M. (1975) *Bull. Acad. Pol. Sci., Ser. Sci., Math., Astron. Phys. XXIII*, 367–372.
Kim, Y., Grable, J. C., Love, R., Greene, P. J., & Rosenberg, J. M. (1990) *Science 249*, 1307–1309.
Lycksell, P. O., Gräslund, A., Claesens, F., McLaughlin, L. W., Larsson, U., & Rigler, R. (1987) *Nucleic Acids Res. 15*, 9011–9025.
McConnell, B., & Politowski, D. (1984) *Biophys. Chem. 20*, 135–148.
McLaughlin, L. W., Benseler, F., Gräser, E., Piel, N., & Scholtissek, S. (1987) *Biochemistry 26*, 7238–7245.
McLaughlin, L. W., Leong, T., Benseler, F., & Piel, N. (1988) *Nucleic Acids Res. 16*, 5631–5644.
Millar, D. P., & Sowers, L. C. (1990) *Proc. SPIE-Int. Soc. Opt. Eng. 1204*, 656–662.
Muccio, D. D., Waterhous, D. V., Fish, F., & Brouillette, C. G. (1992) *Biochemistry 31*, 5560–5567.
Nerdal, W., Hare, D. R., & Reid, B. R. (1989) *Biochemistry 28*, 10008–10021.
Nordlund, T. M. (1990) in *Nonlinear Optics and Ultrafast Phenomena* (Alfano, R. R., & Rothberg, L., Eds.) pp 83–88, Nova Publishing, New York.
Nordlund, T. M., Andersson, S., Nilsson, L., Rigler, R., Gräslund, A., & McLaughlin, L. W. (1989) *Biochemistry 28*, 9095–9103.
Nordlund, T. M., Wu, P., Andersson, S., Nilsson, L., Rigler, R., Gräslund, A., McLaughlin, L. W., Gildea, B. (1990) *Proc. SPIE-Int. Soc. Opt. Eng. 1204*, 344–353.
Nordlund, T. M., Xu, D., & Evans, K. O. (1993) *Biochemistry 32*, 12090–12095.
Preisler, R. S., Mandal, C., Englander, S. W., Kallenbach, N. R., Howard, F. B., Frazier, J., & Miles, H. T. (1981) in *Biomolecular Stereodynamics* (Sarma, R. H., Ed.) pp 405–415, Adenine Press, New York.
Preisler, R. S., Mandal, C., Englander, S. W., Kallenbach, N. R., Frazier, J., Miles, H. T., & Howard, F. B. (1984) *Biopolymers 23*, 2099–2125.
Rosenberg, J. M., McClarin, J. A., Frederick, C. A., Wang, B.-C., & Grable, J. (1986) in *Structure, Dynamics and Function of Biomolecules* (Ehrenberg, A., Rigler, R., Gräslund, A., & Nilsson, L., Eds.) pp 255–259, Springer-Verlag, Heidelberg.
Smagowicz, J., & Wierzchowski, K. L. (1974) *J. Lumin. 8*, 210–232.
Sowers, L. C., Fazakerly, G. V., Eritja, R., Kaplan, B. E., & Goodman, M. F. (1986) *Proc. Natl. Acad. Sci. U.S.A. 83*, 5434–5438.
Thomas, G. A., Kubasek, W. L., Peticolas, W. L., Greene, P., Grable, J., & Rosenberg, J. M. (1989) *Biochemistry 28*, 2001–2009.
Ward, D. C., Reich, E., & Stryer, L. (1969) *J. Biol. Chem. 244*, 1228–1237.
Wartell, R. M., & Benight, A. S. (1985) *Phys. Reports 126*, 67–107.
Westhof, E., & Moras, D. (1987) in *Structure, Dynamics and Function of Biomolecules* (Ehrenberg, A., Rigler, R., Gräslund, A., & Nilsson, L., Eds.) pp 208–211, Springer-Verlag, Heidelberg.
Wilcoxon, J., Schurr, J. M., Wartell, R. M., & Benight, A. S. (1984) *Biochemistry 23*, 1137–1139.
Wu, P., Nordlund, T. M., McLaughlin, L. W., & Gildea, B. (1990) *Biochemistry 29*, 6508–6514.